Phosphorous-doped $CoTe_2$ nanowires as an effective electrocatalyst for bipolar membrane-assisted water splitting in a coupled acid-alkaline water electrolyzer

Isilda Amorim[a,b], Junuyan Xu[a], Nan Zhang[a], Ana Araújo[a,c], Fátima Bento[b] and Lifeng Liu[a,*]

[a]*International Iberian Nanotechnology Laboratory (INL), Avenida Mestre Jose Veiga, 4715-330 Braga, Portugal*
[b]*Centre of Chemistry, University of Minho, Gualtar Campus, Braga, 4710-057, Portugal*
[c]*Laboratory of Catalysis and Materials (LSRE-LCM), Faculdade de Engenharia Universidade do Porto, Rua Dr. Roberto Frias, 4200-465 Porto, Portugal*

[*]Corresponding author.
E-mail address: lifeng.liu@inl.int (L. Liu)

Highlights

- Phosphorous-doped $CoTe_2$ electrode was prepared to use as bifunctional catalyst for HER and OER;
- The doping strategy seems to enhance the electrocatalytic activity of $CoTe_2$ for both HER and OER, when compared with the undoped $CoTe_2$;
- Using a bipolar membrane in an acid-alkaline coupled water electrolyzer and P-$CoTe_2$ as anode and cathode, it is possible to accomplish water electrolysis at 1.72 V to deliver 10 mA cm^{-2};
- The voltage needed to afford 10 mA cm^{-2} can be significantly reduced to 1.01 V, using a "irregular" bipolar membrane, due to assistance of electrochemical neutralization.

Graphical Abstract

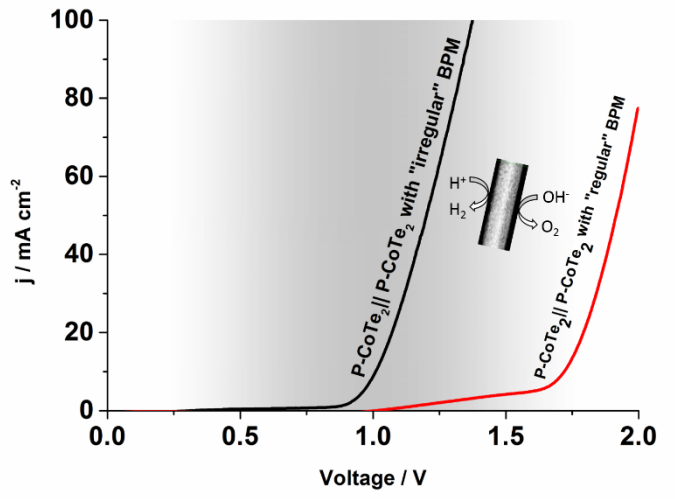

ABSTRACT

Electrochemical water splitting has been recognized as a sustainable and environmentally-friendly way for producing hydrogen fuel. To make electrolyzed hydrogen economically competitive, significant effort has recently been made to developing cheap and efficient earth-abundant electrocatalysts. Notwithstanding substantial progress, the operational voltage of water splitting in a single electrolyte system is still high, even if highly efficient electrocatalysts are used to catalyze the hydrogen evolution (HER) and oxygen evolution reactions (OER). Taking into account that the HER and the OER are thermodynamically favorable in different pH values, in this work we demonstrate that using a bipolar membrane and a facile doping method in which phosphorous can be doped into $CoTe_2$ electrodes, we can accomplish water splitting in acid-alkaline dual electrolytes with an onset voltage as low as 1.09 V, and a voltage of 1.72 V to deliver 10 mA cm^{-2}. Moreover, is also demonstrated that using an "irregular" BPM the voltage needed to reach 10 mA cm^{-2} can be reduced to 1.01 V, due to the assistance of electrochemical neutralization resulted from the unintentional crossover of the electrolytes. The water electrolysis can be sustained for at least 100 h without obvious degradation.

Keywords: P-doped $CoTe_2$ nanowires; bipolar membrane; water splitting; hydrogen evolution reaction; oxygen evolution reaction

1. Introduction

The aggravation of the energy crisis and environmental pollution has increased the concerns on the utilization of clean and sustainable energy in order to replace the fossil fuels. One attractive alternative to fossil fuels is the clean energy carrier hydrogen (H_2) since it holds higher specific energy compared with other fuels and water splitting offers an environmental friendly way for its production, especially if the electric power comes from renewable sources [1]. However, the utilization of H_2 for large scale applications is constrained by the high costs of water electrolyzers and by the high energy demand required (1.4−1.6 V) to catalyze the reaction with electrolysis currents of 10 mA cm^{-2}, larger than the theoretical voltage requirement (1.23 V), owing to the high overpotentials from the half reactions of hydrogen (HER) in the cathode and oxygen evolution reaction (OER) in the anode [2-6].

The precious platinum group metal (PGM) electrocatalysts are usually employed on proton-exchange-membrane water electrolysis (PEMWE), such iridium (Ir) or ruthenium (Ru) to catalyze the OER and platinum (Pt) to catalyze the HER [7]. Although, due to the recent research efforts, Pt-free HER catalysts have been reported for PEMWE [8-10], the noble-metal-free OER catalysts active in acidic environments is still a challenge. Thus, alkaline water electrolysis (AWE), in comparison with PEMWE, offers a big benefit since the use of these noble materials can be avoided. However, this technology suffers with high overpotentials and low current densities therefore the overall performance remains unsatisfactory [11].

Given that thermodynamically the overpotentials are decreased in acidic conditions for HER and in alkaline conditions for OER it's possible to break the pH incompatibilities of the two electrolytes in an electrolyzer comprising acid-alkaline dual solutions separated by a bipolar membrane (BPM) that will allow the minimization of the potential required to split water. This

would enable the water electrolysis to be catalyzed with low-cost and earth-abundant materials.

A BPM is a polymer membrane composed by a cation-exchange membrane (CEM) that is permselective to cations (e.g, H^+) joined to an anion-exchange membrane (AEM) that is permselective to anions (e.g, OH^-)[12, 13]. The BPMs have been recently employed in photoelectrochemical (PEC) water splitting, showing the ability of perform the OER in the anodic compartment, in alkaline conditions and the HER in the cathodic compartment of a cell, in acidic solution [14, 15].

Besides of system design to overcome the thermodynamic barriers of water splitting, electrocatalysts engineering is other strategy to lower the voltage requirement for H_2 production. In recent years, doping has been widely used as an effective approach to enhance the catalytic performance. For instance, doping with an additional transition metal [16], other metals such aluminum [17] or a non-metallic element (such N, S, P) [18-23] have been reported to boost the intrinsic activity of catalysts in water electrolysis.

Herein, we developed phosphorous-doped $CoTe_2$ nanowires (NWs), dropped-cast on carbon paper (CP), here denominated as P-$CoTe_2$, to use as bifunctional electrocatalyst for both electrode reactions and explore the use of a commercially available Fumasep BPM (Fumatech, more details shown **Table S1**) in a coupled configuration with acid-alkaline dual solutions.

The acid-alkaline coupled water electrolyzer can deliver a current density of 10 mA cm^{-2} at 1.72 V, that can be reduced to 1.01 V when using a “irregular” BPM where unintentional crossover among the electrolytes occurs, that allow the assistance of electrochemical neutralization. Moreover, we demonstrate that the “irregular” BPM based electrolyzer is capable to sustain a stable water electrolysis for at least 100 h at 10 mA cm^{-2} showing its promising alternative to conventional proton and anion exchange membrane water electrolysis.

2. Materials and Methods

2.1. Materials

Sodium tellurite (Na_2TeO_3), oleylamine (98%), sodium hydroxide (NaOH), sulfuric acid (H_2SO_4) and sodium hypophosphite (NaH_2PO_2) were purchased from Sigma-Aldrich. Cobalt chloride hexahydrate ($CoCl_2.6H_2O$) was purchased from PanReac. All reagents were used without further purification in this work. Deionized water (DI), from a Millipore system (18.2 MΩ cm), was used for solutions preparation.

2.2. Synthesis of P-$CoTe_2$ nanowires

The cobalt telluride ($CoTe_2$) NWs were synthesized by a hydrothermal method. Firstly, 0.11075 g of Na_2TeO_3 was dissolved on 38 mL oleylamine with 2 mL of water. After continuously sonication for 1 h, 0.11825 g of $CoCl_2.6H_2O$ was added and sonication for another 1 h was done. The resultant solution was transferred to a 50 mL Teflon-lined stainless-steel autoclave. The autoclave was then sealed and maintained at 180 °C for 3 h in an oven. After cooling down to room temperature, the solution was centrifuged at 9000 rpm and rinsed several times with ethanol-cyclohexane mixture (volume ratio, 1/4).

Subsequently, the P-$CoTe_2$ NWs were obtained by phosphorization of the $CoTe_2$ powders. Typically, 65 mg of $CoTe_2$ NWs were loaded on a ceramic boat with 650 mg of NaH_2PO_2 placed 2−3 cm away from the $CoTe_2$ powders. Afterwards, the ceramic boat was put into a tube furnace, with the NaH_2PO_2 placed on the upstream side, wherein high-purity N_2 (99.999 %) was purged for 1 h to remove air. Then the furnace was heated to 300 ºC at a ramping rate of 5 ºC min^{-1} and maintained at this temperature for 2 h. Finally, the furnace was naturally cooled down to room temperature. A constant N_2 flow was maintained throughout the whole process.

2.3. Materials Characterization

The sample morphology was examined by a field-emission scanning electron microscope (FE-SEM, FEI Quanta 650 FEG) equipped with an INCA 350 spectrometer for energy dispersive X-ray spectroscopy (EDX). Microstructure and composition of samples were characterized by a transmission electron microscope (TEM, FEI Titan ChemiSTEM 80-200) operating at 200 keV. Powder X-ray diffraction (XRD) measurements were carried out on a Panalytical X'Pert PRO diffractometer at 45 kV and 40 mA, using Cu K_α radiation (λ = 1.540598 Å) and a PIXcel detector. The Bragg-Brentano configuration was applied to acquire patterns in the 2θ range of 20-80°.

X-ray photoelectron spectroscopy (XPS) data were acquired on an ESCALAB 250 instrument with Al K_α X-rays (1489.6 eV).

2.4. Electrode preparation and HER/OER electrochemical measurements

The catalyst ink was prepared dispersing 5 mg of catalysts into 1 mL of ethanol contaning 50 µL of nafion (Sigma, 5 wt %). To preprare electrodes for a catalytic test, 400 µL of catalyst ink was drop-cast on CP substrat with an exposed area of 1 cm^2 leading to a loading density of *ca.* 2 mg cm^{-2}. The Pt/C (20 wt%) or RuO_2 catalyst were also prepared on CP substrate with the same loading for comparison reasons. The electrode was then dried at room temperature naturally in air. All electrochemical measurements were carried out in a typical three-electrode system at room temperature using a Biologic VMP-3 potentiostat/galvanostat. The CP loaded with the catalyst, a graphite rod (for HER) or Pt wire (for OER) and a saturated calomel electrode (SCE) were utilized as working, counter, and reference electrodes, respectively. The SCE reference was calibrated prior to each measurement in H_2-saturated 0.5 M H_2SO_4 solution using a clean Pt wire as the working electrode. Unless otherwise stated, all potentials are reported versus the reversible hydrogen electrode (RHE), by converting the measured potentials *vs* SCE in accordance with the following formula:

$$E_{RHE} = E_{SCE} + 0.059 \times pH + 0.244 \quad (1)$$

The HER activity was performed in 0.5 M H_2SO_4 and 1.0 M NaOH, and the OER activity was done in 1.0 M NaOH. Cyclic voltammetry (CV) was performed at 5 mV/s and an *iR*-correction of 85% was applied to compensate the potential drop between the working and reference electrodes. Electrochemical impedance spectroscopy (EIS) measurements were carried out at a d.c. voltage of 1.55 V *vs* RHE for OER and −0.21 V or −0.125 *vs* RHE for HER (in NaOH or H_2SO_4, respectively) in the frequency range of 0.01 – 105 Hz with a 10 mV amplitude sinusoidal perturbation. The catalytic stability of the catalysts was assessed at a constant current density of 10 mA cm^{-2} for OER and −10 mA cm^{-2} for HER, at room temperature.

2.5. Overall water splitting performance measurements

For the acid-alkaline coupled water electrolyzer, two pieces of symmetric P-$CoTe_2$ electrodes (1 cm^2) were utilized as cathode and anode, respectively, and a piece of BPM (130-160 μm, Fumasep FBM; Fumatech) was sandwiched between the two Teflon compartments. NaOH (1.0 M, pH= 13.6) and H_2SO_4 (0.5 M, pH = 0.3) were supplied as the anolyte and catholyte, respectively. LSV curves were recorded at a scan rate of 5 mV/s with *iR*-correction (85%). For comparison, commercial RuO_2 and Pt/C (20 wt%) were also used as OER and HER catalysts, respectively, and tested in the same coupled configuration. The alkaline water electrolysis performance of the P-$CoTe_2$ electrodes was investigated in a two-compartment Teflon cell with two pieces of symmetric 1.0 cm^2 P-$CoTe_2$ placed in the anodic and cathodic compartments, separated by an AEM (15 μm, FAAM-15; Fumatech). 1.0 M NaOH was used as a single electrolyte. LSV curves were recorded at a scan rate of 5 mV/s with *iR*-correction (85%).

2.6.Turnover frequency (TOF) calculation

For OER and HER, the TOF values (s^{-1}) were calculated assuming that every metal atom was involved in the catalysis, which represents the lower limit of the TOF [24]:

OER: $TOF = \frac{j}{4nF}$ (2)

HER: $TOF = \frac{j}{2nF}$ (3)

Where j is the current (A) at a given overpotential, F is the Faraday constant (96485 C mol^{-1}) and n (mol) is the mole number of metals loaded on the CP electrode which was determined by the inductively coupled plasma optical emission spectroscopy (ICP-OES) analysis. The ICP-OES was performed on an ICPE-9000 spectrometer (Shimadzu). Specifically, 2.5 mg of catalysts were dispersed in 2 mL of aqua regia. Subsequently, the acidic solution was diluted in a 100 mL volumetric flask. The analysis was performed three times using *ca.* 10 mL of solution each time to obtain an average value.

3. Results and Discussion

The P-$CoTe_2$ NWs were obtained upon phosphorization of $CoTe_2$ NWs obtained by hydrothermal synthesis. The structure and morphology of the $CoTe_2$ was analysed by XRD and SEM. As shown on **Fig. S1a**, the SEM confirmed the nanowires morphology while the XRD (**Fig. S2**) shows that $CoTe_2$ nanowires comprised a mixture of crystal phases, where the predominately phase seems to be cubic $CoTe_2$, mixed with monoclinic (TeO_3)(TeO_2) and cubic Te. After phosphorous doping by a phosphorization process, using NaH_2PO_2, the nanowires morphology was retained (**Fig S1b**), but they seem thicker. On the other hand, XRD after phosphorization (**Fig.1a**) show that the oxide phase disappears, and the P-$CoTe_2$ NWs appears to be composed mostly by orthorhombic $CoTe_2$ with a mixture of cubic Te. The surface chemical composition and chemical state of P-$CoTe_2$ were determined by XPS. In the Co2p spectrum (**Fig. 1b**), the $Co2p_{3/2}$ can be well fitted into one peak at 778.5 eV attributed to the binding energy of $CoTe_2$ [25, 26]. **Fig. 1c** shows the high-resolution Te 3d XPS spectra, where the peaks at 572.5 and 582.9 eV are consistent with the binding energy of Te $3d_{5/2}$ and Te $3d_{3/2}$, respectively, as a consequence of the formation of metallic Te. The

remaining two peaks at 574.5 and 584.8 eV can be attributed to oxide state (TeO_x) of Te [27, 28]. However, the TeO_x signal does not necessarily mean that the material is composed of TeO_x, since the XRD result show that the bulk phase is $CoTe_2$. Therefore, the presence of TeO_x may result from the oxidation of the generated P-$CoTe_2$ in air [27] so may be only present on the outermost surface. As far as the P 2p XPS spectrum is concerned (**Fig. 1d**), two peaks appearing at 128.9 and 129.8 eV can be assigned to P $2p_{3/2}$ and P $2p_{1/2}$, respectively, which is characteristic of Co-P bonds [29, 30]. This further demonstrates that P was successfully doped into $CoTe_2$ NWs. Additionally, a strong peak at 133.9 eV is observed, arising from the P-O bond due to the air exposure of P-$CoTe_2$ [31].

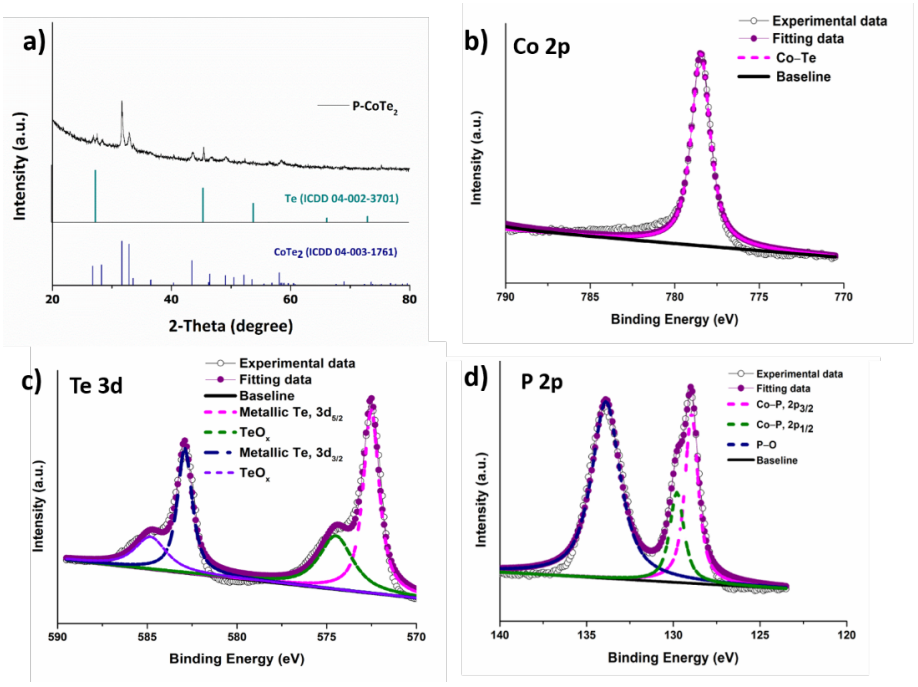

Fig. 1. Surface chemical composition and chemical state of P-$CoTe_2$. (a) X-ray diffraction pattern of P-$CoTe_2$ electrode. For reference, the standard power diffraction patterns of Te (ICCD 04-002-3701) and $CoTe_2$ (ICCD 04-003-1762) are also given. (b) Co 2p; (c) Te 3d; (d) P 2p X-ray photoelectron spectroscopy spectra of the P-$CoTe_2$ electrode.

The microstructure and composition of P-$CoTe_2$ were further examined by TEM. As illustrated in **Fig. 2a**, the TEM image shows that the P-$CoTe_2$ NWs consisted of many porous crystal grains. A high-resolution TEM (HRTEM) image is illustrated in **Fig. 2b** and **Fig. 2c**, where different lattice

fringes of crystallized domains can be clearly resolved. In **Fig. 2b** the measured interplanar distance of *ca.* 0.314 nm were assigned to the lattice spacing of (101) of $CoTe_2$ (ICDD 04-003-1761) while that of *ca.* 0.320 nm, corresponds to the (111) crystal plane of Te (ICDD 04-002-3701). Other lattices fringes corresponding to the (210) and (120) crystal plane of $CoTe_2$ (ICDD 04-003-1761), with interplanar distances of 0.248 and 0.270 nm, respectively, were also resolved (**Fig. 2c**). Extensive TEM-EDX analysis confirmed that P-$CoTe_2$ consist of Co, Te and P elements (**Fig. 2d**) and the Cu signal comes from the copper grid used. High-angle annular dark field scanning TEM (HAADF-STEM) observation show that the elements Co, Te and P are uniformly distributed over the whole NW. The oxygen signal should originate from surface oxidation due exposure of samples to air.

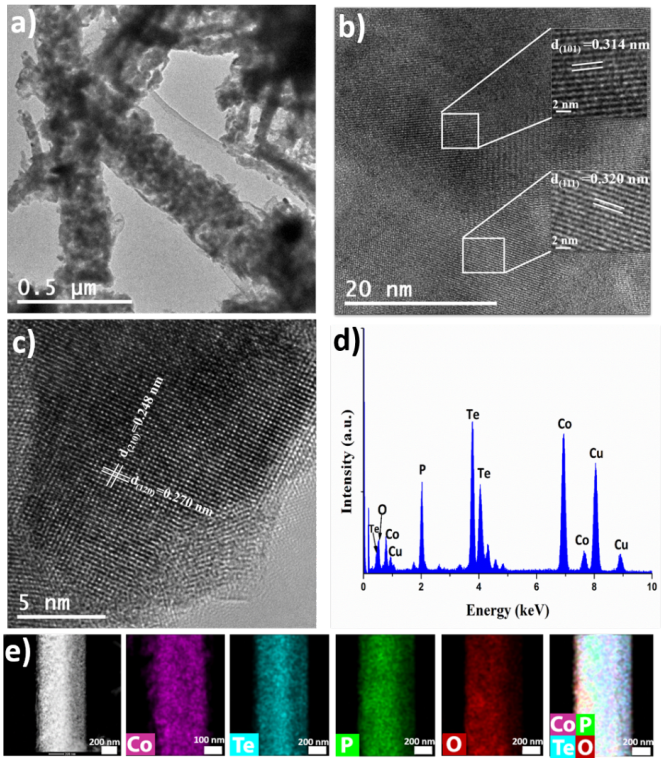

Fig.2. Microstructure characterization of P-$CoTe_2$ nanowires. (a) Low-magnification transmission electron microscopy image. (b), (c) High-resolution transmission electron microscopy image of an individual P-$CoTe_2$ nanowire at different zones. (d) TEM-EDX spectrum. (e) HAADF-STEM image and elemental maps of Co, Te, P, O, and their overlay.

The electrocatalytic performances of P-$CoTe_2$ and $CoTe_2$ catalysts toward the HER in H_2SO_4 and NaOH and toward OER in NaOH were evaluated on CP substrates, using a three-electrode system. For comparison, RuO_2, Pt/C and CP were tested under the same conditions. The carbon paper itself is catalytically inactive toward the HER in both pH conditions as well for OER since do not show cathodic current density, only if high potentials are applied (e.g. > - 0.55 V *vs* RHE for HER in 1.0 M NaOH and > 1.8 V *vs* RHE for OER). It is clear that P-$CoTe_2$ NWs exhibit better HER and OER performance than $CoTe_2$, indicating that doping with P significantly improves the catalytic activity (**Fig. 3**). For HER, the overpotential needed to deliver a current density of 10 mA cm^{-2} (η_{10}) for P-$CoTe_2$ is 138 mV in H_2SO_4 while the $CoTe_2$ does not show any performance (**Fig. 3a**). This result is favourably compared with P-$CoTe_2$/C nanoparticles (η = 159 mV), reported recently by Wang *et al*. [19]. In NaOH, the P-$CoTe_2$ exhibits a η_{10} = 178 mV much lower than η_{10} = 479 mV obtained for $CoTe_2$ which show negligible activity (**Fig. 3b**). These HER results obtained suggested that the phosphorous-doped $CoTe_2$ is more active than other reported telluride catalysts (**Table S2**).

Likewise, the electrodes were also tested for OER in alkaline conditions (**Fig. 3c**). The η_{10} value of P-$CoTe_2$ (η_{10} = 346 mV) is slightly inferior than $CoTe_2$ (η_{10} = 362 mV). Note that the overpotential of P-$CoTe_2$ catalyst is comparable to and even smaller than those of many reported telluride OER catalysts (**Table S3**). As shown on **Fig. 3d**, the HER and OER stability of P-$CoTe_2$ was assessed by chronopotentiometry. Only a small increase in the potential of the catalyst was observed after 14 h of continuous electrolysis. The reactions kinetics was analysed by Tafel plots. For both reactions, the Tafel slope also decreases after doping $CoTe_2$ with phosphorous, as shown on **Fig. 3e**, indicating that the doping accelerates the kinetic reactions. The Tafel slope of 97 mV dec^{-1} and 112 mV dec^{-1} obtained for P-$CoTe_2$ in HER conditions at H_2SO_4 and NaOH respectively, is in the range of 40-120 mV dec^{-1}, showing that the HER process follows the Volmer-Heyrosvky

mechanism [32]. As well, the lower value of Tafel slope obtained for P-$CoTe_2$ in OER (44 mV dec^{-1}) suggests a fast kinetic for the electron transfer. The fast HER and OER kinetics for the P-doped material was also confirmed by EIS measurements. As shown on **Fig. 3f**, the charge transfer resistance (R_{ct}) of P-$CoTe_2$ is substantially lower than that of undoped $CoTe_2$, implying that P doping enhances the charge transfer ability during HER and OER. The intrinsic HER and OER activity of the materials was further evaluated based on TOF, assuming all transition metal species in the TMPs are catalytically active (i.e., the lower limit). The TOF values are compared in **Fig. S3** calculated at η = 350 mV. The results show that the TOF value is greatly improved after phosphorous doping, indicating that P-$CoTe_2$ is intrinsically more active than $CoTe_2$ for both reactions.

The overall water electrolysis performance of two symmetric P-$CoTe_2$ electrodes was tested first in 1.0 M NaOH, using a two-compartment Teflon cell separated by a Fumatech AEM (denoted as P-$CoTe_2$||AEM||P-$CoTe_2$), simulating the anion exchange membrane water electrolysis. Was found that a voltage (E_{10}) of 1.80 V is needed to deliver 10 mA cm^{-2} (black trace in **Fig. 4b**).

Further, using the same electrodes pairs, the water splitting performance was tested in a acid-alkaline dual electrolytes configuration, in the same Teflon cell separated by a BPM, as shown on **Fig. 4a** (denoted as P-$CoTe_2$ in 1.0 M NaOH||BPM||P-$CoTe_2$ in 0.5 M H_2SO_4). In this configuration (blue trace in **Fig. 4b**), water electrolysis can be accomplished with E_{10} = 1.72 V which is slightly better than the above-mentioned anion exchange membrane water electrolysis. In addition, the onset voltage using the BPM configuration (E_{onset}= 1.09 V) is much lower than that using AEM configuration (E_{onset}= 1.47 V). Extensive electrochemical tests using different batches of Fumasep BPMs were made and most of them showed nicely reproducible results. However, there was one batch of BPM, were the acid-alkaline coupled water electrolysis could be accomplished with

significantly lower external voltage using the same P-$CoTe_2$ pair as electrodes (**Fig. 4c**).

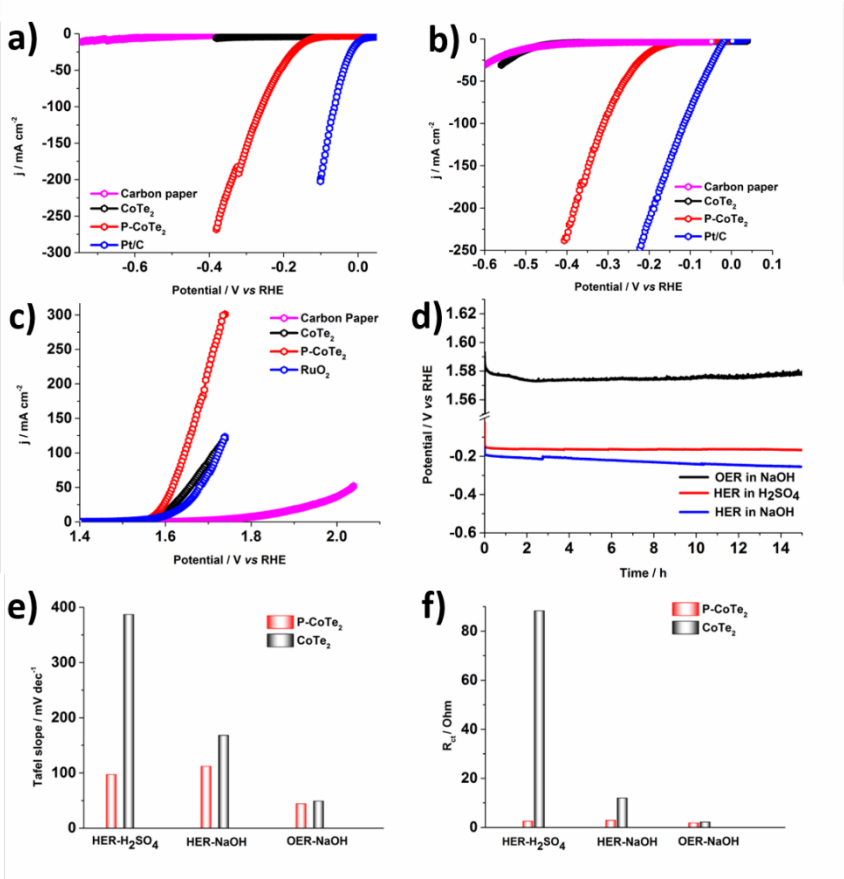

Fig.3. Electrocatalytic performance of the P-$CoTe_2$ electrode toward HER and OER at room temperature. *iR*-corrected HER polarization curves of a piece of carbon paper, commercial Pt/C (20 wt%) and the P-$CoTe_2$ and $CoTe_2$ electrodes recorded at a scan rate of 5 mV/s in (a) 0.5 M H_2SO_4 and (b) 1.0 M NaOH. (c) *iR*-corrected OER polarization curves of a piece of carbon paper, commercial RuO_2 and the P-$CoTe_2$ and $CoTe_2$ electrodes recorded at a scan rate of 5 mV/s in 1.0 M NaOH. (d) Chronopotentiometric curves of the P-$CoTe_2$ electrode recorded at a constant anodic current density of 10 mA cm^{-2} in 1.0 M NaOH and at a constant cathodic current density of −10 mA cm^{-2} in 0.5 M H_2SO_4 and 1.0 M NaOH. (e) Tafel slope comparison between the P-$CoTe_2$ and $CoTe_2$ electrodes. (f) R_{ct} comparison between the P-$CoTe_2$ and $CoTe_2$ electrodes.

Remarkably, a E_{onset} = 0.78 V and a E_{10}= 1.01 V was obtained and even at high current density of 100 mA cm^{-2} a low voltage of 1.37 V can be achieved. The water electrolysis attained at such unusual low external voltage could be interpreted as the energy from secondary neutralization reaction between the OH^- and the H^+, in the anodic and cathodic compartment, respectively, that

occurs in parallel to water electrolysis, as reported by other groups [33-35]. This neutralization occurs from the unintentional crossover in the BPM (such BPM is denoted as an "irregular" BPM) that it is an exergonic process and consequently can lower the energy required for water splitting [36]. A simple calculation can be done in order to testify that water electrolysis in this case is assisted by electrochemical neutralization. For instance, the measured voltage needed to reach 10 mA cm^{-2} is only 1.01 V for P-$CoTe_2$ pair separated by an "irregular" BPM. Though, taking the electrochemical neutralization into account (0.059/pH x (13.6-0.3)pH = 0.79 V), the actually required voltage would be around 1.80 V (1.01 + 0.79) which is comparable to the E_{10} value of the electrolyzer separated by a "regular" BPM (*i.e.* without neutralization, E_{10}= 1.72 V). It is worth mentioning that the reproducibility of the tests were confirmed by doing a larger number of tests using the "irregular" BPM, even though this piece of "irregular" BPM was made unintentionally by the supplier. The stability of the water electrolyzer separated by a "regular" and an "irregular" BPM using the P-$CoTe_2$ as bifunctional catalysts was assessed at a constant current density of 10 mA cm^{-2}. For comparison, the stability of P-$CoTe_2$ using the AEM in 1.0 M NaOH and the BPM-based water electrolysis using RuO_2 to catalyze OER in 1.0 M NaOH and Pt/C to catalyze HER in 0.5 M H_2SO_4, was also evaluated. As shown on **Fig. 4d** the electrolysis carried out by the RuO_2||Pt/C pair using the "regular" BPM suffers a performance decay in the first 10 h of water splitting and remains approximately constant in the next 90 h. The AEM based electrolyzer can sustain the current density of 10 mA cm^{-2} for at least 100 h with little performance decay, but the cell voltage to maintain the current density is much higher. In contrast, the acid-alkaline coupled water electrolyzer separated by a "regular" BPM (red trace in **Fig. 4d**) can operate at a lower cell voltage in the course of 100 hours while the acid-alkaline coupled water electrolyzer separated by an "irregular" BPM (black trace in **Fig. 4d**) can split water at much inferior voltage, as expected.

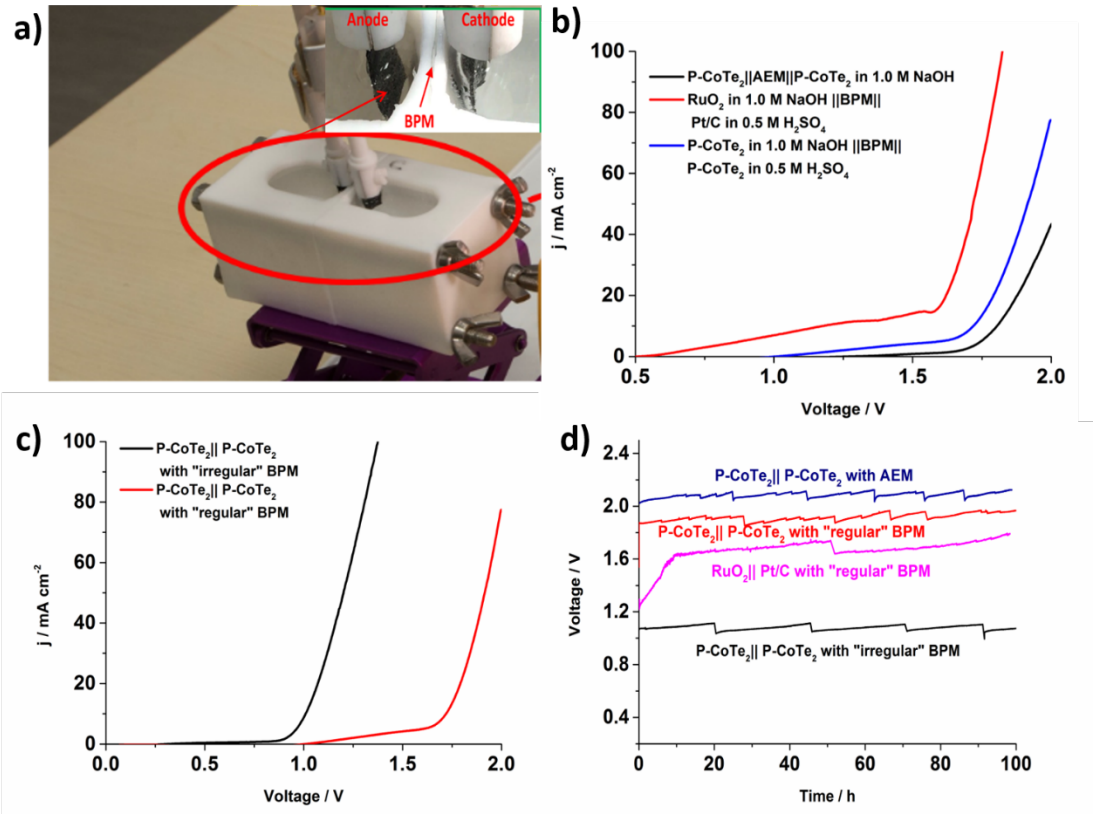

Fig.4. Water electrolysis tests. a) Demonstration of a two-compartment Teflon cell separated by a polymer membrane. b) *iR*-corrected (85%) polarization curve of the bipolar membrane-based acid-alkaline coupled water electrolysis. For comparison, water electrolysis was also tested in a single solution using the same bifunctional electrodes separated by an anion exchange membrane (AEM). c) *iR*-corrected (85%) polarization curve of the acid-alkaline coupled water electrolysis with a "regular" and an "irregular" BPM. d) Catalytic stability of acid-alkaline coupled water electrolysis with a "regular" and an "irregular" BPM. For comparison, the stability of RuO_2 in 1.0 M NaOH||BPM||Pt/C in 0.5 M H_2SO_4, and P-$CoTe_2$||AEM||P-$CoTe_2$ in 1.0 M NaOH were also presented. No *iR* correction was applied.

4. Conclusions

In summary, we have synthetized a P-doped cobalt telluride using a simple hydrothermal method followed by a post-phosphorization process. We investigate the electrocatalytic activity toward HER and OER of the P-doped and undoped $CoTe_2$, and we found that the phosphorous doping can significantly improve the electrocatalytic performance toward HER and OER when compared with that of undoped $CoTe_2$, since lower overpotentials, Tafel slopes and R_{ct} are obtained after doping.

We also demonstrated the overall water splitting in an acid-alkaline coupled water electrolyzer separated by a BPM, using P-$CoTe_2$ bifunctional electrodes. This water electrolyzer needs a voltage of 1.72 V to deliver 10 mA cm^{-2}, but can be accomplished at lower external bias, i.e. 1.01 V at 10 mA cm^{-2}, if an "irregular" BPM with unintentional crossover is used, generating electrochemical neutralization energy, facilitating water splitting and reducing electricity energy consumed. Moreover, this electrolyzer can sustain water splitting for at least 100 h. This study shows great promise for use as an alternative to the state of art AWE and PEMWE, that may facilitates the large-scale production of hydrogen with minimum energy consumption if an "irregular" BPM is applied.

Declaration of Competing Interest

The authors declare that they have no known competing financial interests or personal relationships that could have appeared to influence the work reported in this paper.

Acknowledgments

This work was financially supported by the European Horizon 2020 project "CritCat" under the grant agreement number 686053. Isilda Amorim is thankful for the support to FCT PhD grant SFRH/BD/137546/2018.

Appendix A. Supplementary data

Supplementary data to this article can be found online at https://doi.org/10.1016/j.cej.2021.130454.

References

[1] T.D. Veras, T.S. Mozer, D.D.R.M. dos Santos, A.D. Cesar, Hydrogen: Trends, production and characterization of the main process worldwide, Int J Hydrogen Energ 42 (2017) 2018-2033.
[2] F. Yu, H.Q. Zhou, Y.F. Huang, J.Y. Sun, F. Qin, J.M. Bao, W.A. Goddardiii, S. Chen, Z.F. Ren, High-performance bifunctional porous non-noble metal phosphide catalyst for overall water splitting, Nat Commun 9 (2018).
[3] G. Anandhababu, Y.Y. Huang, D.D. Babu, M.X. Wu, Y.B. Wang, Oriented Growth of ZIF-67 to Derive 2D Porous CoPO Nanosheets for Electrochemical-/Photovoltage-Driven Overall Water Splitting, Adv Funct Mater 28 (2018).
[4] G. Zhang, Y.S. Feng, W.T. Lu, D. He, C.Y. Wang, Y.K. Li, X.Y. Wang, F.F. Cao, Enhanced Catalysis of Electrochemical Overall Water Splitting in Alkaline Media by Fe Doping in Ni3S2 Nanosheet Arrays, Acs Catal 8 (2018) 5431-+.
[5] Y.C. Pi, Q. Shao, P.T. Wang, J. Guo, X.Q. Huang, General Formation of Monodisperse IrM (M = Ni, Co, Fe) Bimetallic Nanoclusters as Bifunctional Electrocatalysts for Acidic Overall Water Splitting, Adv Funct Mater 27 (2017).
[6] J. Yang, Y. Ji, Q. Shao, N. Zhang, Y. Li, X. Huang, A universal strategy to metal wavy nanowires for efficient electrochemical water splitting at pH-universal conditions, Adv Funct Mater 28 (2018) 1803722.
[7] Z.W. Seh, J. Kibsgaard, C.F. Dickens, I.B. Chorkendorff, J.K. Norskov, T.F. Jaramillo, Combining theory and experiment in electrocatalysis: Insights into materials design, Science 355 (2017).
[8] X. Wang, F. Li, W.Z. Li, W.B. Gao, Y. Tang, R. Li, Hollow bimetallic cobalt-based selenide polyhedrons derived from metal-organic framework: an efficient bifunctional electrocatalyst for overall water splitting, J Mater Chem A 5 (2017) 17982-17989.
[9] C. Lin, Z.F. Gao, J.H. Yang, B. Liu, J. Jin, Porous superstructures constructed from ultrafine FeP nanoparticles for highly active and exceptionally stable hydrogen evolution reaction, J Mater Chem A 6 (2018) 6387-6392.
[10] J.S. Moon, J.H. Jang, E.G. Kim, Y.H. Chung, S.J. Yoo, Y.K. Lee, The nature of active sites of Ni2P electrocatalyst for hydrogen evolution reaction, J Catal 326 (2015) 92-99.
[11] F.M. Sapountzi, J.M. Gracia, C.J. Weststrate, H.O.A. Fredriksson, J.W. Niemantsverdriet, Electrocatalysts for the generation of hydrogen, oxygen and synthesis gas, Prog Energ Combust 58 (2017) 1-35.
[12] M.B. McDonald, S. Ardo, N.S. Lewis, M.S. Freund, Use of Bipolar Membranes for Maintaining Steady-State pH Gradients in Membrane-Supported, Solar-Driven Water Splitting Chemsuschem 7 (2014) 3021-3027.
[13] N.M. Vargas-Barbosa, G.M. Geise, M.A. Hickner, T.E. Mallouk, Assessing the Utility of Bipolar Membranes for use in Photoelectrochemical Water-Splitting Cells, Chemsuschem 7 (2014) 3017-3020.
[14] K. Sun, R. Liu, Y.K. Chen, E. Verlage, N.S. Lewis, C.X. Xiang, A Stabilized, Intrinsically Safe, 10% Efficient, Solar-Driven Water-Splitting Cell Incorporating Earth-Abundant Electrocatalysts with Steady-State pH Gradients and Product Separation Enabled by a Bipolar Membrane, Adv Energy Mater 6 (2016).
[15] J.S. Luo, D.A. Vermaas, D.Q. Bi, A. Hagfeldt, W.A. Smith, M. Gratzel, Bipolar Membrane-Assisted Solar Water Splitting in Optimal pH, Adv Energy Mater 6 (2016).
[16] L. Zhong, Y.F. Bao, X. Yu, L.G. Feng, An Fe-doped NiTe bulk crystal as a robust catalyst for the electrochemical oxygen evolution reaction, Chem Commun 55 (2019) 9347-9350.
[17] M. Wang, W.J. Zhang, F.F. Zhang, Z.H. Zhang, B. Tang, J.P. Li, X.G. Wang, Theoretical Expectation and Experimental Implementation of In Situ Al-Doped CoS2 Nanowires on Dealloying-Derived Nanoporous Intermetallic Substrate as an Efficient Electrocatalyst for Boosting Hydrogen Production, Acs Catal 9 (2019) 1489-1502.
[18] X. Xie, R.J. Yu, N. Xue, A. Bin Yousaf, H. Du, K. Liang, N. Jiang, A.W. Xu, P doped molybdenum dioxide on Mo foil with high electrocatalytic activity for the hydrogen evolution reaction, J Mater Chem A 4 (2016) 1647-1652.

[19] Q. Wang, K. Cui, J. Li, Y. Wu, Y. Yang, X. Zhou, G. Ma, Z. Yang, Z. Lei, S. Ren, Phosphorus-doped CoTe2/C nanoparticles create new Co-P active sites to promote the hydrogen evolution reaction, Nanoscale 12 (2020) 9171-9177.
[20] J.R. Zeng, M.Y. Gao, Q.B. Zhang, C. Yang, X.T. Li, W.Q. Yang, Y.X. Hua, C.Y. Xu, Y. Li, Facile electrodeposition of cauliflower-like S-doped nickel microsphere films as highly active catalysts for electrochemical hydrogen evolution, J Mater Chem A 5 (2017) 15056-15064.
[21] J.F. Chang, K. Li, Z.J. Wu, J.J. Ge, C.P. Liu, W. Xing, Sulfur-Doped Nickel Phosphide Nanoplates Arrays: A Monolithic Electrocatalyst for Efficient Hydrogen Evolution Reactions, Acs Appl Mater Inter 10 (2018) 26303-26311.
[22] Q.W. Zhou, Z.H. Shen, C. Zhu, J.C. Li, Z.Y. Ding, P. Wang, F. Pan, Z.Y. Zhang, H.X. Ma, S.Y. Wang, H.G. Zhang, Nitrogen-Doped CoP Electrocatalysts for Coupled Hydrogen Evolution and Sulfur Generation with Low Energy Consumption, Adv Mater 30 (2018).
[23] Z. Liu, X. Yu, H.G. Xue, L.G. Feng, A nitrogen-doped CoP nanoarray over 3D porous Co foam as an efficient bifunctional electrocatalyst for overall water splitting, J Mater Chem A 7 (2019) 13242-13248.
[24] J.Y. Xu, D.H. Xiong, I. Amorim, L.F. Liu, Template-Free Synthesis of Hollow Iron Phosphide Phosphate Composite Nanotubes for Use as Active and Stable Oxygen Evolution Electrocatalysts, Acs Applied Nano Materials 1 (2018) 617-624.
[25] G.J. Zhang, K.H. Liu, J.S. Zhou, Cobalt telluride/graphene composite nanosheets for excellent gravimetric and volumetric Na-ion storage, J Mater Chem A 6 (2018) 6335-6343.
[26] K. Wang, Z.G. Ye, C.Q. Liu, D. Xi, C.J. Zhou, Z.Q. Shi, H.Y. Xia, G.W. Liu, G.J. Qiao, Morphology-Controllable Synthesis of Cobalt Telluride Branched Nanostructures on Carbon Fiber Paper as Electrocatalysts for Hydrogen Evolution Reaction, Acs Appl Mater Inter 8 (2016) 2910-2916.
[27] Q.R. Shi, C.Z. Zhu, D. Du, J. Wang, H.B. Xia, M.H. Engelhard, S. Feng, Y.H. Lin, Ultrathin dendritic IrTe nanotubes for an efficient oxygen evolution reaction in a wide pH range, J Mater Chem A 6 (2018) 8855-8859.
[28] M. Liu, X.Q. Lu, C. Guo, Z.J. Wang, Y.P. Li, Y. Lin, Y. Zhou, S.T. Wang, J. Zhang, Architecting a Mesoporous N-Doped Graphitic Carbon Framework Encapsulating CoTe2 as an Efficient Oxygen Evolution Electrocatalyst, Acs Appl Mater Inter 9 (2017) 36146-36153.
[29] Z.J. Sun, B.H. Lv, J.S. Li, M. Xiao, X.Y. Wang, P.W. Du, Core-shell amorphous cobalt phosphide/cadmium sulfide semiconductor nanorods for exceptional photocatalytic hydrogen production under visible light, J Mater Chem A 4 (2016) 1598-1602.
[30] A.P. Grosvenor, S.D. Wik, R.G. Cavell, A. Mar, Examination of the Bonding in Binary Transition-Metal Monophosphides MP (M = Cr, Mn, Fe, Co) by X-Ray Photoelectron Spectroscopy, Inorg Chem 44 (2005) 8988-8998.
[31] X.Y. Zhang, W.L. Gu, E.K. Wang, Wire-on-flake heterostructured ternary Co0.5Ni0.5P/CC: an efficient hydrogen evolution electrocatalyst, J Mater Chem A 5 (2017) 982-987.
[32] X. Zhang, X.L. Yu, L.J. Zhang, F. Zhou, Y.Y. Liang, R.H. Wang, Molybdenum Phosphide/Carbon Nanotube Hybrids as pH-Universal Electrocatalysts for Hydrogen Evolution Reaction, Adv Funct Mater 28 (2018).
[33] Y. Li, J. Chen, P. Cai, Z. Wen, An electrochemically neutralized energy-assisted low-cost acid-alkaline electrolyzer for energy-saving electrolysis hydrogen generation, J Mater Chem A 6 (2018) 4948-4954.
[34] H. Zou, J. Chen, Y. Fang, J. Ding, W. Peng, R. Liu, A dual-electrolyte based air-breathing regenerative microfluidic fuel cell with 1.76 V open-circuit-voltage and 0.74 V water-splitting voltage, Nano Energy 27 (2016) 619-626.
[35] J. Xu, I. Amorim, Y. Li, J. Li, Z. Yu, B. Zhang, A. Araujo, N. Zhang, L. Liu, Stable overall water splitting in an asymmetric acid/alkaline electrolyzer comprising a bipolar membrane sandwiched by bifunctional cobalt-nickel phosphide nanowire electrodes, Carbon Energy (2020) 1-10.
[36] G. Wang, J. Chen, P. Cai, J. Jia, Z. Wen, A self-supported Ni–Co perselenide nanorod array as a high-activity bifunctional electrode for a hydrogen-producing hydrazine fuel cell, J Mater Chem A 6 (2018) 17763-17770.